Supplementary information for

# Towards scalable reductive etherification of 5-hydroxymethyl-furfural through iridium-zeolite-based bifunctional catalysis

Zehui Sun [a], Mugeng Chen [a], Kaizhi Wang [a], Chen Chen [a], Jiachen Fei [a], Wendi Guo [a], Conglin Zhu [a],Heyong He [a], Yongmei Liu [a,*], Yong Cao [a,*]

[a] Shanghai Key Laboratory of Molecular Catalysis and Innovative Materials, Department of Chemistry, Fudan University, Shanghai 200433, China

* Corresponding author. E-mail: *ymliu@fudan.edu.cn (Yongmei Liu),* yongcao@fudan.edu.cn *(Yong Cao)*

## 1. Materials and Chemicals

All reagents and chemicals were of analytical grade and used as received without any further purification in this study. Detailed description of the reagents and chemicals are showed below. Support materials of Zeolites like H-ZSM-5-11.5, H-ZSM-5-15, H-ZSM-5-40, H-ZSM-5-140, H-beta-12.5, H-MCM-22, H-Y-2.6 and H-MOR were supplied by Zeolyst. A380 fumed $SiO_2$ was supplied by Evonik. Amberlyst-15 was supplied by Aladdin. Metal precursors $H_2IrCl_6{\cdot}xH_2O$, $(NH_4)_2IrCl_6$, $H_2PtCl_6{\cdot}xH_2O$, $PdCl_2$ and $RuCl_3{\cdot}xH_2O$ was supplied by Aladdin. Alkali metal hydroxides such as LiOH, NaOH and KOH were supplied by sinopharm. Substrates, reactants, products and solvents like 5-hydroxymethylfurfural (HMF), 2,5-bis(hydroxymethyl)furan (BHMF), 2,5-bis(methoxymethyl)furan (BMMF), 5-(methoxymethyl)furan-2-carbaldehyde (MMF), furfural, 2,5-diformylfuran, (DFF), benzaldehyde (BA), methanol, ethanol and isopropanol (IPA) were supplied by Aladdin. (5-(Dimethoxymethyl)furan-2-yl)methanol (DMMF) was supplied by bidepharm. helium (99.999%), nitrogen (99.999%), hydrogen/argon (5 vol% $H_2$/Ar), ammonia/helium (10 vol% $NH_3$/He) were purchased from Air Liquide.

## 2. Catalyst preparation

### *2.1 Preparation of alkali-modified zeolites support*

Alkali-modified zeolites were synthesized via an alkali-metal grafting method in alcoholic media as described earlier by Javier et al..[1] Typically, 1 g of zeolite (H-ZSM-5-11.5, H-beta-12.5 and H-Y-2.6) without further pretreatment was introduced into a solution (30 mL) of the desired concentration n (0-0.5) M of alkali metal hydroxide (MOH: LiOH, NaOH and KOH) in methanol at room temperature,

and stirred at 500 rpm for 10 min, filtered, washed thoroughly with methanol 3 times with 100 mL, and dried at 60 $^{o}$C and calcined (5 $^{o}$C min$^{-1}$, 550 $^{o}$C, 6 h) to obtain xM-Zeolite, where x represents the mass contents of M in the catalyst .

*2.2 Preparation of alkali-modified zeolites supported Ir catalyst*

All the catalysts were prepared by impregnation facilitated by evaporation according to our previous work.[2] Typically, for the preparation of 0.75Ir/0.8Na-ZSM-5, 15.6 mg of $H_2IrCl_6$ was first dissolved in 10 mL deionized water with 0.1 M HCl. Subsequently, 1 g of 0.8Na-ZSM-5 support was introduced slowly into this solution. After stirring at 25 $^{o}$C for 3 h, the obtained slurry was vigorously stirred at 80 $^{o}$C for 4 h. After that, samples were separated from the slurry by reduced pressure distillation. Finally, the solid samples were dried under vacuum at 25 $^{o}$C for 12 h and then reduced in 5 vol% $H_2$/Ar (80 mL/min) at 500 $^{o}$C for 2 h to obtain 0.75Ir/0.8Na-ZSM-5.

*2.3 Preparation of alkali-modified zeolites supported other metal (Pd, Pt, Ru) catalyst*

All the catalysts were prepared by impregnation facilitated by evaporation according to our previous work. Briefly, a certain amount of $H_2PtCl_6$, $PdCl_2$ and $RuCl_3$ was first dissolved in 10 mL deionized water with 0.1 M HCl. Subsequently, 1 g of 0.8Na-ZSM-5 support was introduced slowly into this solution. After stirring at 25 $^{o}$C for 3 h, the obtained slurry was vigorously stirred at 80 $^{o}$C for 4 h. After that, samples were separated from the slurry by reduced pressure distillation. Finally, the solid samples were dried under vacuum at 25 $^{o}$C for 12 h and then reduced in 5 vol% $H_2$/Ar (80 mL/min) at 500 $^{o}$C for 2 h to obtain corresponding samples.

*2.4 Preparation of referential Lewis acidic Sn-beta catalyst*

Sn-beta catalyst with a Sn loading of 4% was prepared via a reported Solid-state ion-exchange (SSIE) method.[3] Typically, Commercial zeolite H-beta (Zeolyst) was dealuminated via treatment in concentrated $HNO_3$ solution (13 M) at 110 $^{o}$C for 4 h (50 mL·g$^{-1}$ (zeolite)) by three times. SSIE was performed by ball-milling of appropriate amount of tin(II)acetate with the required amount of dealuminated H-beta zeolite for 30 min at 60 rpm. Samples were calcined in an air flow at 550 $^{o}$C for 6 h with a ramp rate of 10 $^{o}$C·min$^{-1}$.

**3. Catalytic performance evaluation**

In order to eliminate the influence of diffusion, all solid samples were ground and granulated to 100-200 mesh, and vacuum dried at 150 °C for 3 h before reaction.

*3.1 Direct etherification of BHMF to BMMF*

Typically, 4 mmol BHMF (512 mg) and 5 mL of methanol were placed in a 15 mL oven-dried round-bottom tube with steady magnetic stirring (800 rpm) at 50 °C under an ambient atmosphere of air. The reaction was started by the addition of a calculated amount of catalyst and the mixture was allowed to stir for required reaction time. After completion of the reaction, dodecane (50 μL), used as an internal standard, was added to the reaction mixture. For determining conversion and selectivity, filtrate was analyzed by GC (Agilent 7820A gas chromatograph with FID detector and 30 m×0.32 mm×0.25 μm HP-INNOWax capillary column).

*3.2 Reductive etherification of HMF to BHMF*

Typically, calculated amount of catalyst, 4 mmol (11.3 wt.%) or 8 mmol (22.6 wt.%) HMF and 5 mL of methanol were placed in a 25 mL Hastelloy-C high pressure reactor (Beijing Century Senlang Experimental Apparatus Co., Ltd.; contain a stainless-steel sampling tube with filter). Then, the reactor was charged with hydrogen to given pressure of 1 MPa. The reactor was heated to targeted temperature of 50 $^{o}$C and kept stirring for a certain period of time. Upon completion, the reaction liquid was taken from the reactor through sampling tube. The conversion and selectivity were determined by GC using dodecane as an internal standard. The initial TOF was measured at HMF conversion below 20% based on total metal atoms.

*3.3 Reduction of HMF in 1,4-dioxane for TOF calculation*

Typically, calculated amount of catalyst, 4 mmol or 8 mmol HMF and 5 mL of 1,4-dioxane were placed in a 25 mL Hastelloy-C high pressure reactor. Then, the reactor was charged with hydrogen to 1 MPa. The reactor was heated to 50 $^{o}$C and kept stirring for a certain period of time. Upon completion, the reaction liquid was taken from the reactor through sampling tube. The conversion and selectivity were determined by GC using dodecane as an internal standard. The initial TOF was measured at HMF conversion below 20% based on total metal atoms.

*3.4 Reductive etherification of HMF to BHMF in flow-reaction mode*

The reactions were performed on a ThalesNano® Phoenix Flow Reactor (Figure S11). An HPLC pump was used for substrate solution introduction. $H_2$ was introduced by gas module. The liquid and gas were intensively mixed by liquid-gas mixer and flowed by up-flow through the reaction column. The system pressure was regulated by a back-pressure valve. While the product solution was mainly

collected in product container, the change valve can bypass the product container to sample the reaction mixture.

In most cases, the HMF conversion, product selectivity, carbon balance and Turnover Number (TON) were calculated according to the following equations:

$$\text{Conversion}\ (\%) = \frac{HMF_{input} - HMF_{residue}}{HMF_{input}} \times 100\%$$

$$\text{Selectivity}\ (\%) = \frac{mole\ of\ Product_i}{\sum_i^n mole\ of\ Product_i} \times 100\%$$

$$\text{Carbon Balance}\ (C.B.)\ (\%) = \frac{Carbon_{products\ in\ liquid\ phase}}{Carbon_{conversed\ HMF} + Carbon_{conversed\ MeOH}} \times 100\%$$

$$Turnover\ Number\ (TON) = \frac{mole\ of\ yielded\ BMMF}{mole\ of\ total\ Ir\ site}$$

TOF was defined as the number of HMF molecules that was conversed per metal site of corresponding catalyst per unit of time ($h^{-1}$) at HMF conversion below 20%, and was calculated according to the following equations:

$$Turnover\ Frequency\ (\text{TOF})\ (h^{-1}) = \frac{mole\ of\ conversed\ HMF}{mole\ of\ total\ Ir\ sites * reaction\ time}$$

$TOF_X$ was defined as the number of yielded molecules that was produced via certain reaction pathway X, including -C=C- hydrogenation, -C-O hydrogenolysis and -C=O hydrogenation pathway, per metal site of [Ir], [Pd], [Pt] and [Ru] catalyst per unit of time ($h^{-1}$) at HMF conversion below 20%, and was calculated according to the following equations:

$$Turnover\ Frequency'\ (\text{TOF'})\ (h^{-1}) = \frac{mole\ of\ yileded\ products\ via\ certain\ pathway}{mole\ of\ total\ metal\ sites * reaction\ time}$$

where X includes -C=C- hydrogenation, -C-OH hydrogenolysis and -C=O hydrogenation.

## 4. Catalyst characterization

In this study, these samples were comprehensively characterized to understand their physical and chemical properties. Elemental analysis (EA) of samples was conducted with a PerkinElmer inductively coupled plasma optical emission spectrometer (ICP-OES) Optima 8300 DV.

Before transferred into the TEM chamber, the samples dispersed with ethanol were deposited onto copper grid and then quickly moved into the vacuum evaporator. The size distribution of the metal nanoparticles was determined by measuring about 150 random particles in the images. High angle annular dark-field scanning transmission electron microscopy (HAADF-STEM) images were obtained on a Tecnai $G_2$ F20 S-Twin electron microscope, operating at 200 kV.

X-ray diffraction (XRD) was operated on a Bruker D8 Advance X-ray diffractometer using the Ni-filtered Cu-$K_\alpha$ radiation source at 40 kV and 40 mA.

AutoiChem II 2920 high performance automatic chemisorption instrument made by Micromeritics was used for $NH_3$-TPD and $H_2$-TPR analyses. The 100 mg sample was placed in a quartz tube, which was pretreated at 300 °C for 2 hours in argon atmosphere and then reduced to 50 °C. After saturated with adsorbed ammonia, 30 mL·min$^{-1}$ He air was used to purge until the physically adsorbed ammonia was completely desorbed, and then the temperature program was performed at a rate of the rate for 10 °C·min$^{-1}$ to 600 °C. The removed $NH_3$ components were detected by OmniStar (QMS-200) mass spectrometer, and *m/e* = 16 was selected as MS signal of $NH_3$ desorption to avoid the interference of $H_2O$ molecules (*m/e* = 18, 17).

Fourier-transform infrared spectroscopy (FT-IR) was carried out with a Nicolet iS10 FT-IR spectrometer equipped with a DTGS detector, in the range 400-4000 cm$^{-1}$, by applying an optical resolution of 0.4 cm$^{-1}$. The samples were investigated by using the KBr pellet technique.

Sample surface acidity was also assessed by pyridine adsorbed Fourier transform infrared spectrometry (Py−FTIR) using a Thermo-Fisher Nicolet iS50 spectrometer, which was used and the test conditions were shown: samples were pretreated at 300 °C vacuum for 2 h to remove the adsorbed moisture from the samples. Spectra were recorded at the range of 4000-1000 cm$^{-1}$ at 25, 150 and 300 °C. For the quantification of Brønsted and Lewis acid sites, integral molar extinction coefficients (IMEC) of 1.67 and 2.22 cm/mol, respectively, were adopted.

The DRIFT spectra of chemisorbed CO were recorded in an in-situ diffuse reflectance cell (Harick Scientific) equipped with a $CaF_2$ window on a Nicolet 6700 spectrometer (Thermo Fisher Scientific), using an Hg-Cd-Te (MCT-A) detector. Each spectrum was collected for 64 scans at a resolution of 4 cm$^{-1}$. The sample (ca. 20 mg) was pretreated in the cell with flowing high-purity He (20 mL/min) at 250 °C for 0.5 h and subsequently in-situ reduced at desired temperature to obtain the catalyst in reduced form. The temperature was then lowered to 15 °C for CO chemisorption. After collecting a

background spectrum of the sample under the He flow, the cell was switched to flowing 1 vol% CO/He (20 mL/min) for CO adsorption for 1 h, followed by purging with He. Spectra were taken at varying time intervals during this purging stage to make sure that gaseous CO was essentially absent in the cell. The collected spectra were subtracted from the sample background spectra in He to obtain the spectra for chemisorbed CO.

XPS spectra were recorded on an AXIS Supra X-ray photoelectron spectrometer (Kratos Analytical Ltd.) using a monochromatized Al Kα radiation source. The binding energy was calibrated by the C 1s peak at 284.8 eV.

Thermal-gravimetric analysis (TGA): TGA of the catalysts after reaction was carried out on a Q600 SDT thermogravimetric analyzer (TA Instruments). The air-dried samples of about 10 mg were balanced under air flow (30 $mL \cdot min^{-1}$), and then heated in air from room temperature to 900 $^{o}C$ at a heating rate of 10 $°C \cdot min^{-1}$.

## 5. Supplementary data (Table S1-9/Fig. S1-14)

Table S1 Catalytic performances of direct etherification of BHMF to BMMF over different acidic catalyst support

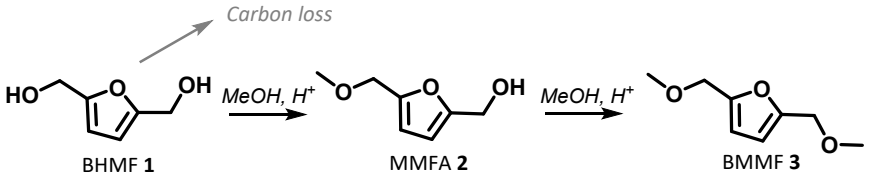


| Entry | Catalyst | Conv. (%) | Yield of BMMF (%) | Yield of MMFA (%) | C.B. (%) |
|---|---|---|---|---|---|
| 1 | H-ZSM-5-11.5 | 100 | 66 | 10 | 76 |
| 2 | H-ZSM-5-15 | 92 | 54 | 14 | 76 |
| 3 | H-ZSM-5-40 | 65 | 27 | 20 | 82 |
| 4 | H-ZSM-5-140 | 17 | 6 | - | 89 |
| 5 | H-Beta-12.5 | 85 | 23 | 36 | 74 |
| 6 | H-MCM-22-20 | 23 | 5 | - | 82 |
| 7 | H-Y-2.6 | 53 | 25 | 5 | 77 |
| 8 | H-MOR | 36 | 14 | 5 | 83 |
| 9 | Amberlyst-15 | 100 | 4 | 63 | 67 |
| 10 | A380-$SiO_2$ | 16 | - | - | 94 |
| 11 | Sn-beta | 15 | - | - | 85 |

Reaction conditions: 100 mg catalyst, BHMF 4 mmol, 5 mL MeOH, 60 $^{o}$C, 2 h, under 0.1 MPa of nitrogen atmosphere, determined by GC with dodecane as internal standard. (H-ZSM-5 showed relatively higher activity and selectivity towards BMMF formation. Among a series of H-ZSM-5 with different Si to Al ratios, specifically, H-ZSM-5-11.5 exhibited the best catalytic performance. Besides, in most cases, reaction proceeded in a low carbon balance manner. Notably, Lewis acid catalyst Sn-beta, synthesized according to reported method, barely catalyzed the etherification of BHMF.)

Table S2 Comparison of catalytic performances of direct etherification of BHMF with methanol over reported system and Na-ZSM-5 in this work

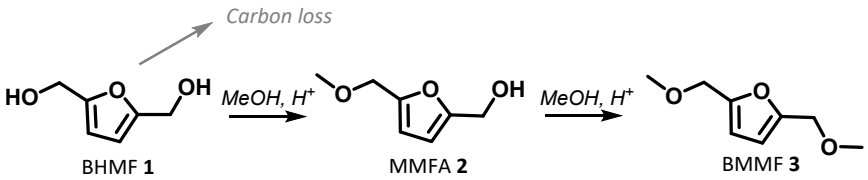


| Entry | Catalyst | Temp. (°C) | Time (h) | Conc. (M) | Conv.(%) | Yield(%) | Ref. |
|---|---|---|---|---|---|---|---|
| 1 | 0.8Na-ZSM-5 (This work) | 60 | 6 | 0.8 | 100 | 91 | *This work* |
| 2 | Purolite CT269DR | 40 | 24 | 0.8 | 100 | 99 | *Arico group*[4] |
| 3 | Glu-TsOH-Ti | 70 | 8 | 0.2 | 100 | 89 | *Saha group*[5] |
| 4 | Amberlyst-15 | 60 | 10 | 1.2 | 99 | 57 | *Lee group*[6] |
| 5 | H-ZSM-5-12.5 | 100 | 3 | 0.8 | - | 70 | *Mu group*[7] |
| 6 | Sn-ZSM-5-25 | 65 | 8 | 0.08 | 100 | 95 | *Zhang group*[8] |

Table S3 Results of direct etherification of BHMF to BMMF over a series of alkaline exchanged (Li, Na, K) catalysts

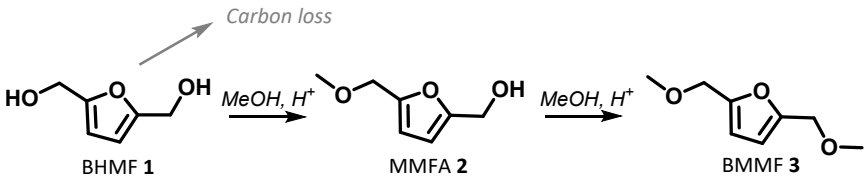


| Entry | Catalyst | Conv. (%) | Yield of BMMF (%) | Yield of MMFA (%) | C.B. (%) |
|---|---|---|---|---|---|
| 1 | H-ZSM-5-11.5 | 100 | 66 | 10 | 76 |
| 2 | 0.1Li-ZSM-5-11.5 | 100 | 63 | 18 | 81 |
| 3 | 0.8Li-ZSM-5-11.5 | 100 | 55 | 34 | 89 |
| 4 | 1.5Li-ZSM-5-11.5 | 34 | 14 | 13 | 93 |
| 5 | 0.1Na-ZSM-5-11.5 | 100 | 62 | 21 | 83 |
| 6 | 0.8Na-ZSM-5-11.5 | 97 | 54 | 36 | 93 |
| 7[a] | 1.5Na-ZSM-5-11.5 | 100 | 91 | 1 | 92 |
| 8[a] | 0.75Ir/0.8Na-ZSM-5 | 100 | 89 | 4 | 93 |
| 9 | 1.5Na-ZSM-5-11.5 | 35 | 17 | 16 | 98 |
| 10 | 0.1K-ZSM-5-11.5 | 100 | 65 | 20 | 85 |
| 11 | 0.8K-ZSM-5-11.5 | 94 | 52 | 30 | 88 |
| 12 | 1.5K-ZSM-5-11.5 | 31 | 16 | 10 | 95 |

Reaction conditions: 100 mg catalyst, BHMF 4 mmol, 5 mL MeOH, 60 $^{o}$C, 2 h, under 0.1 MPa of nitrogen atmosphere, determined by GC with dodecane as internal standard. a: reaction for 6 h. (We found that the introduction of proper amount of alkali metals including Li, Na and K can generally improve the selectivity towards BMMF formation and decrease humins formation. )

Table S4 Surface Brønsted acid ($BA^{surf}$) density and surface Lewis acid ($LA^{surf}$) density calculated from Py-FTIR

| Entry | Catalyst | Brønsted acid amount (mmol/g) | Lewis acid amount (mmol/g) | Brønsted acid ($BA^{surf}$) density ($nm^{-2}$) | Lewis acid ($LA^{surf}$) density ($nm^{-2}$) |
|---|---|---|---|---|---|
| 1 | H-ZSM-5 | 0.209 | 0.0189 | 0.286 | 0.0259 |
| 2 | 0.8Na-ZSM-5 | 0.144 | 0.236 | 0.197 | 0.323 |
| 3 | 0.75Ir/0.8Na-ZSM-5 | 0.121 | 0.133 | 0.166 | 0.183 |
| 4 | 1.5Na-ZSM-5 | 0.0209 | 0.245 | 0.0286 | 0.336 |

The Brønsted acid ($BA^{surf}$) density was calculated upon the Brønsted acid amount acquired from Py-FTIR and specific surface areas obtained from BET.

Table S5 The influence of pressure and temperature for reductive etherification of HMF to BMMF over 0.75Ir/0.8Na-ZSM-5

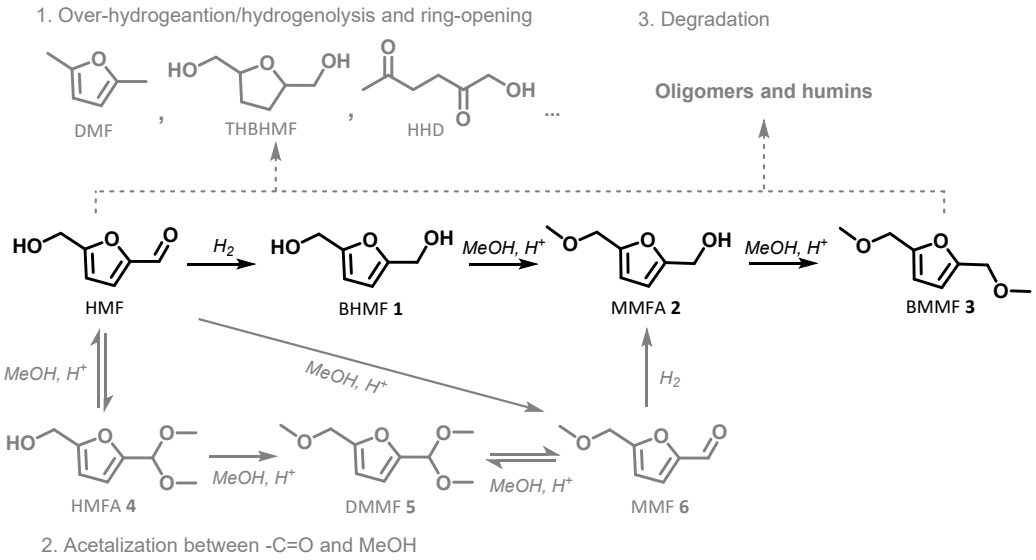


| Entry [a] | Temp. (°C) | Pressure (MPa) | Conv. (%) | Selectivity (%)[b] | | | | | | | Yield (%) | C.B. (%) |
|---|---|---|---|---|---|---|---|---|---|---|---|---|
| | | | | 1 | 2 | 3 | 4 | 5 | 6 | others | | |
| **1** | 50 | 1 | 56 | - | 25 | 75 | - | - | - | - | 42 | 99 |
| **2** | 40 | 1 | 41 | - | 19 | 81 | - | - | - | - | 32 | 99 |
| **3** | 60 | 1 | 68 | 2 | 24 | 72 | - | - | 2 | - | 45 | 95 |
| **4** | 70 | 1 | 82 | 4 | 20 | 62 | 3 | 5 | 4 | 2 | 47 | 93 |
| **5** | 50 | 0.5 | 31 | - | 15 | 85 | - | - | - | - | 26 | 99 |
| **6** | 50 | 2 | 74 | 12 | 33 | 51 | - | - | - | 4 | 36 | 97 |
| **7** | 50 | 3 | 87 | 20 | 12 | 44 | 2 | - | 4 | 18 | 33 | 89 |

[a] Reaction conditions: 4 mmol HMF (504 mg HMF, 0.8 M, 11.3 wt.%), 5 mL MeOH, metal (0.1 mol%), 50 °C, 1 MPa $H_2$, 12 h.

[b] Product 1-6 present: BHMF, MMFA, BMMF, HMFA, DMMF and MMF respectively. Others means over-hydrogenated products including DMF, THBHMF, HHD etc.

With the increase of temperature, the carbon balance drops evidently, which is in concordance with the thermal instability of HMF. With the increase of $H_2$ pressure, the hydrogenation efficiency was solely increased, thus leading to the accumulation of BHMF, which caused the decrease of carbon balance.

Table S6 Basic structure and acidity properties of different samples

| Sample | $V_{micro}$ ($cm^3 \cdot g^{-1}$)[a] | $S_{BET}$ ($m^2 \cdot g^{-1}$)[a] | $S_{ext}$ ($m^2 \cdot g^{-1}$)[a] | Ir amount (wt.%)[b] | Na amount (wt.%)[b] | Acid amount (mmol/g)[c] | Acidity strength distribution (%)[d] | | |
|---|---|---|---|---|---|---|---|---|---|
| | | | | | | | weak | medium | strong |
| H-ZSM-5 | 0.2265 | 442.49 | 93.94 | - | 0.01 | 1.32 | 29 | 39 | 32 |
| 0.1Na-ZSM-5 | - | - | - | - | 0.10 | 1.30 | 31 | 44 | 25 |
| 0.8Na-ZSM-5 | 0.2215 | 444.69 | 76.95 | - | 0.77 | 1.03 | 41 | 42 | 17 |
| 1.5Na-ZSM-5 | 0.2178 | 437.67 | 71.89 | - | 1.49 | 0.43 | 68 | 32 | 0 |
| 0.3Ir/0.8Na-ZSM-5 | 0.2267 | 434.52 | 76.30 | 0.32 | 0.75 | 0.98 | - | - | - |
| 0.75Ir/0.8Na-ZSM-5 | 0.2338 | 420.41 | 74.18 | 0.74 | 0.80 | 0.96 | 43 | 46 | 11 |
| 1.5Ir/0.8Na-ZSM-5 | - | - | - | 1.56 | 0.79 | 0.92 | - | - | - |
| Used-0.3Ir/0.8Na-ZSM-5 | 0.2106 | 417.44 | 74.05 | 0.31 | 0.74 | 0.97 | - | - | - |

[a] obtained from BET results
[b] obtained from ICP-OES results
[c] calculated from $NH_3$-TPD results
[d] calculated from deconvoluted $NH_3$-TPD results

Table S7 Catalytic performances of reductive etherification of HMF to BMMF over Pd/Na-ZSM-5, Ru/Na-ZSM-5 and Pt/Na-ZSM-5

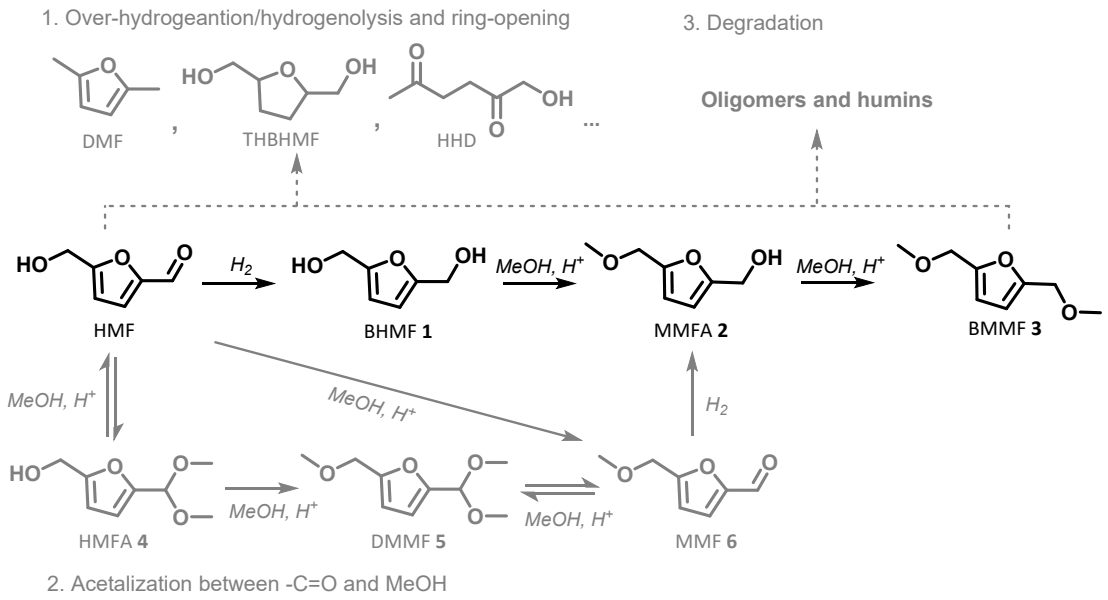


| Entry | Catalyst[a] | Conv. (%) | Select. (%)[b] | | | | | | | Yield of 3 (%) | C.B. (%) |
|---|---|---|---|---|---|---|---|---|---|---|---|
| | | | 1 | 2 | 3 | 4 | 5 | 6 | others | | |
| **1** | Ir/0.8Na-ZSM-5 | 56 | - | 25 | 75 | - | - | - | - | 42 | 99 |
| **2** | Pd/0.8Na-ZSM-5 | 87 | 18 | 21 | 15 | 3 | 2 | - | 41 | 11 | 88 |
| **3** | Pt/0.8Na-ZSM-5 | 77 | 9 | 33 | 55 | 2 | 1 | - | - | 27 | 72 |
| **4** | Ru/0.8Na-ZSM-5 | 82 | 2 | 12 | 11 | 19 | 20 | - | 36 | 8 | 89 |

[a] Reaction conditions: 4 mmol HMF (504 mg HMF, 0.8 M, 11.3 wt.%), 5 mL MeOH, metal (0.1 mol%), 50 °C, 1 MPa $H_2$, 3 h.

[b] Product 1-6 represent: BHMF, MMFA, BMMF, HMFA, DMMF and MMF respectively. Others means over-hydrogenated products including DMF, THBHMF, HHD etc.

Table S8 Comparison of catalytic performances of reductive etherification of HMF with methanol over reported system and 0.75Ir/0.8Na-ZSM-5 in this work

| Entry | Catalyst | Temp. (°C) | $P_{H_2}$ (MPa) | Time (h) | Conc. (M) | Yield(%) | TON | Ref. |
|---|---|---|---|---|---|---|---|---|
| 1 | 0.75Ir/0.8Na-ZSM-5 (This work) | 50 | 1 | 15 | 0.8 | 91 | 5018 (in flow mode) | *This work* |
| 2 | $Pt/Al_2O_3$ + Amberlyst-15 | 60 | 1.4 | 18 | 0.4 | 59 | 400 | *Bell group*[9] |
| 3 | $Cu/SiO_2$ + H-ZSM-5(25) | 120 | 2.5 | 12 | 0.8 | 68 | - | *Mu group*[7] |
| 4 | Cu, CuO-USY | 130 | 2 | 3 | 0.08 | 95 | - | *Lin group*[10] |
| 5 | $Co_3O_4$-100 | 140 | 2 | 1 | 0.1 | 98 | - | *Fu group*[11] |
| 6 | $Ru(OH)_x/ZrO_2$ + Amberlyst-15 | 120/60 | 1.5 | 10 | 0.2 | 50 | 1667 | *Lee group*[6] |
| 7 | $Cu/Al_2O_3$ + hierarchical pore ZSM-5 catalyst | 100 | 2.5 | 3 | 0.4 | 73 | - | *Zhang group*[12] |

Concluded form these results, the utilization of non-noble-metals-based catalysts suffered from elevated temperature and diluted concentration and the employment of strong solid acid catalyst like amberlyst-15 resulted in inferior carbon balance.

Table S9 Catalytic performances of direct etherification/acetalization of HMF in MeOH over different catalysts

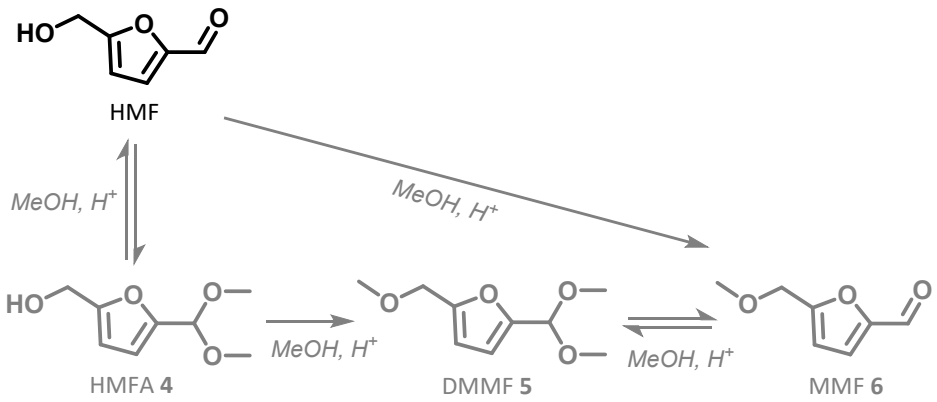


| Entry | Catalyst | Conv. (%) | Yield of HMFA (%) | Yield of DMMF (%) | Yield of MMFA (%) | C.B. (%) |
|---|---|---|---|---|---|---|
| 1 | blank | 11 | 9 | - | - | 98 |
| 2 | H-ZSM-5 | 68 | 27 | 3 | 16 | 78 |
| 3 | 0.8Na-ZSM-5 | 24 | 14 | - | 3 | 93 |
| 4 | 0.75Ir/0.8Na-ZSM-5 | 17 | 8 | - | 3 | 94 |

Reaction condition: 100 mg Catalyst, HMF 4 mmol, 5 mL MeOH, 60 $^{o}$C, under 0.1 MPa of $N_2$ atmosphere 1 h.

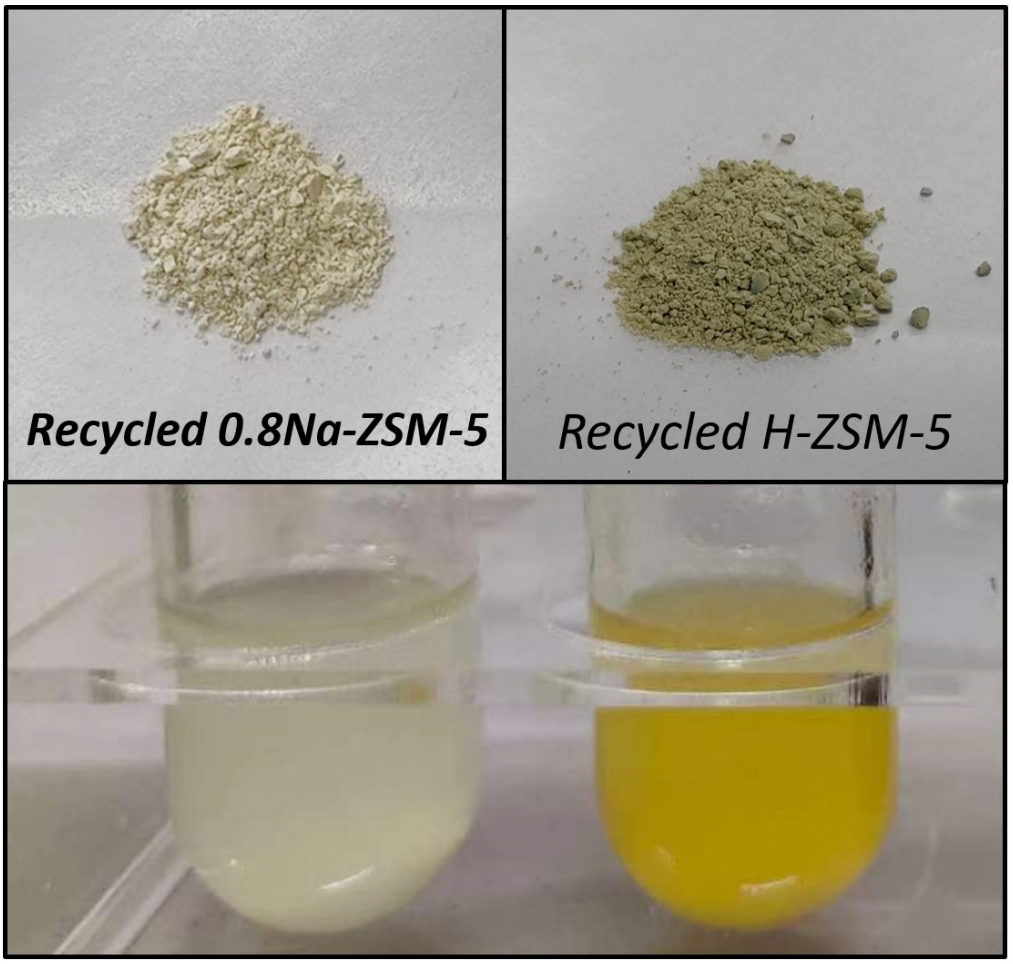


Fig. S1 Photos of spent 0.8Na-ZSM-5 and spent H-ZSM-5 samples.

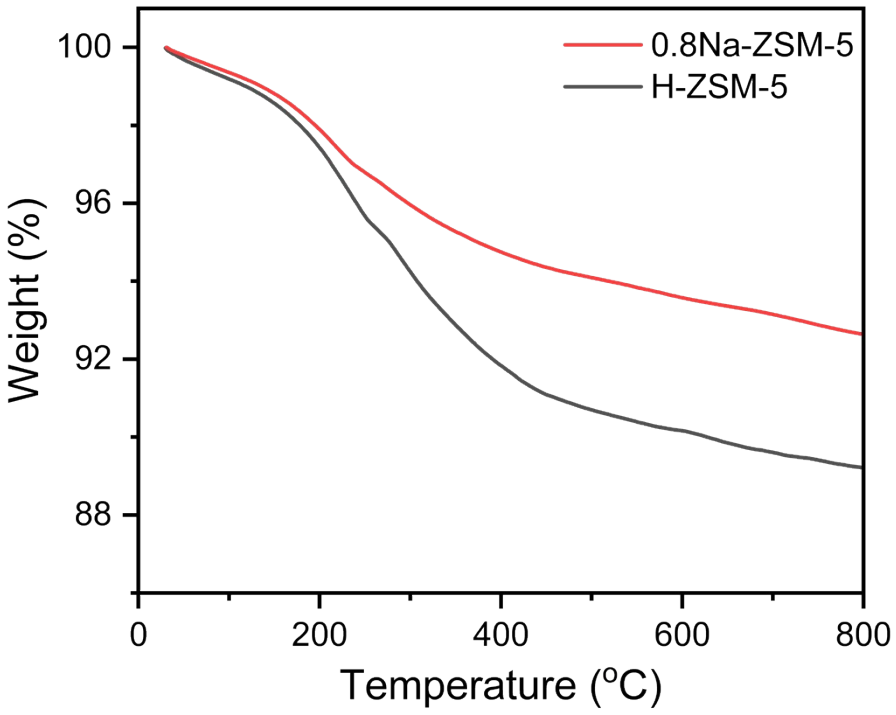


Fig. S2 TG results of spent 0.8Na-ZSM-5 and spent H-ZSM-5 samples after one cycle of etherification reaction.

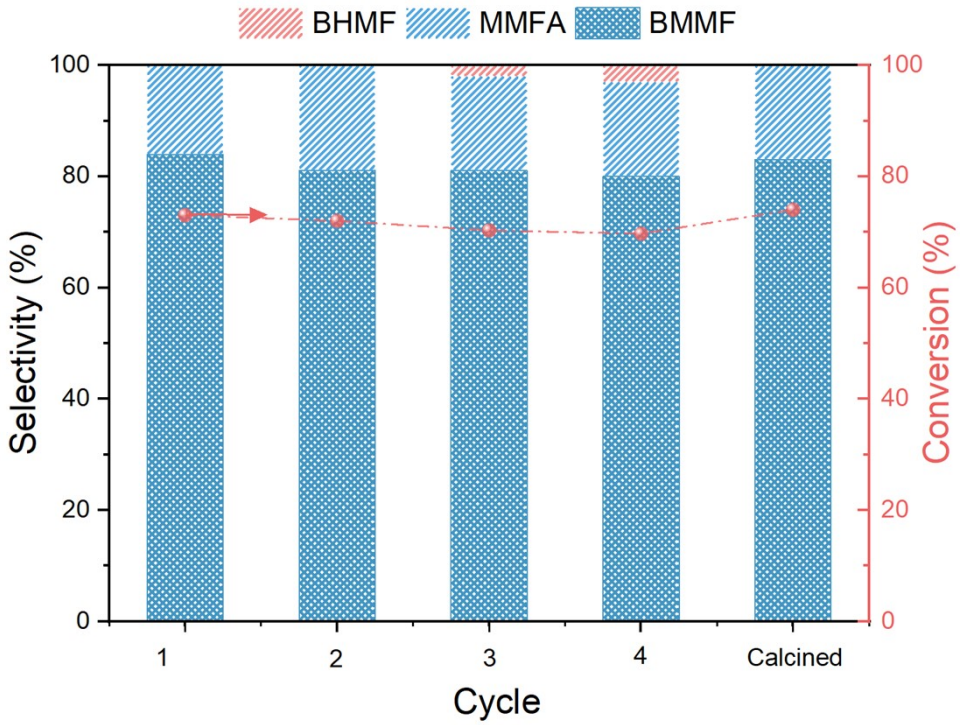


Fig. S3 Recycling results of 0.3Ir/0.8Na-ZSM-5 catalyst. Reaction conditions: 8 mmol HMF, 5 mL MeOH, metal (0.1 mol%), 50 °C, 1 MPa $H_2$, 6 h. (After each batch of reaction, the catalysts were separated, washed with methanol and subsequently dried in oven at 60 °C. For the calcination procedure, the separated catalyst was calcined under air flow at 400 °C for 4 h and subsequently reduced under 5 vol%-$H_2$/Ar flow at 500 °C for 1 h. It is noticed that the activity of 0.3Ir/0.8Na-ZSM-5 was basically recovered after calcination step. Similar procedure was reported by Tomishige group[13].)

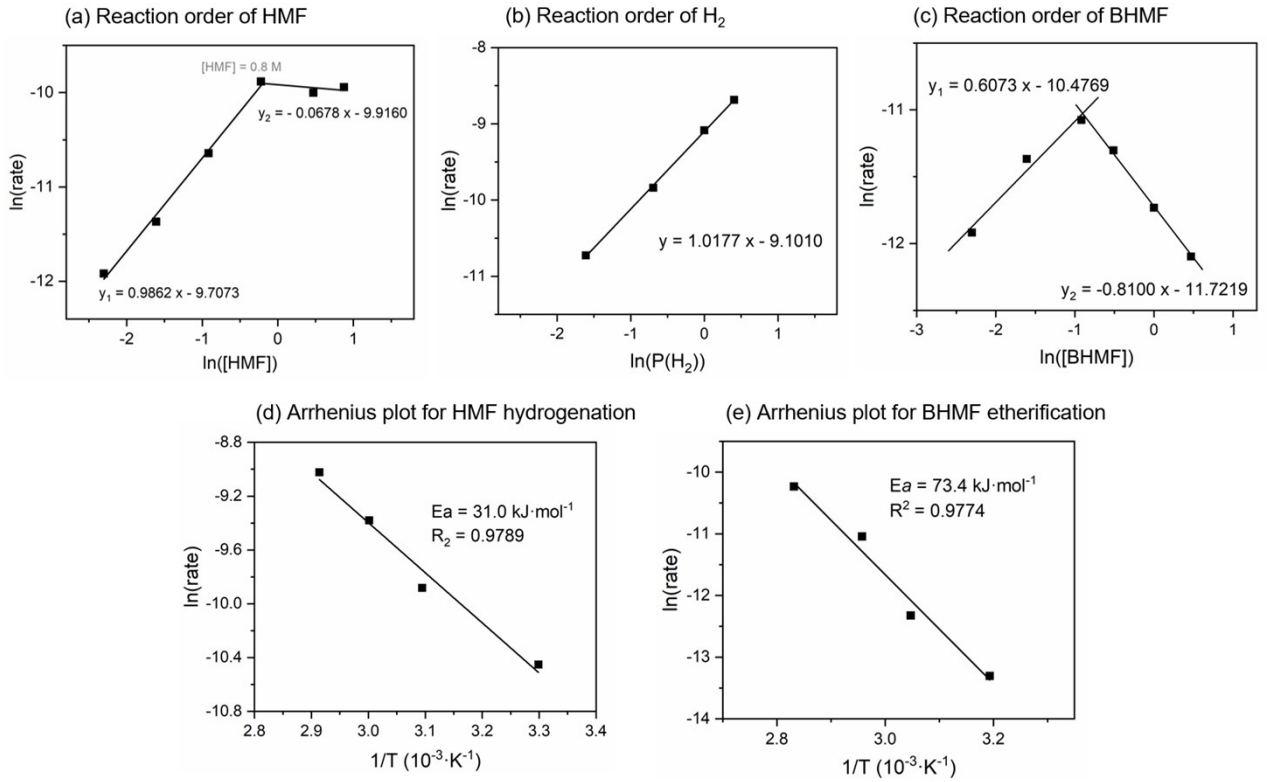


Fig. S4 Plot of ln(rate) versus (a) ln([HMF]), (b) ln([$P(H_2)$]) and (c) ln([BHMF]). Note that a negative order was observed for HMF hydrogenation (ca. -0.06) and BHMF etherification (ca. -0.81), indicating that high concentration of HMF and BHMF is unfavorable for reaction proceeding. Arrhenius plot for 0.75%-Ir/Na-ZSM-5 catalyzed (d) reductive etherification of HMF and (e) etherification of BHMF.

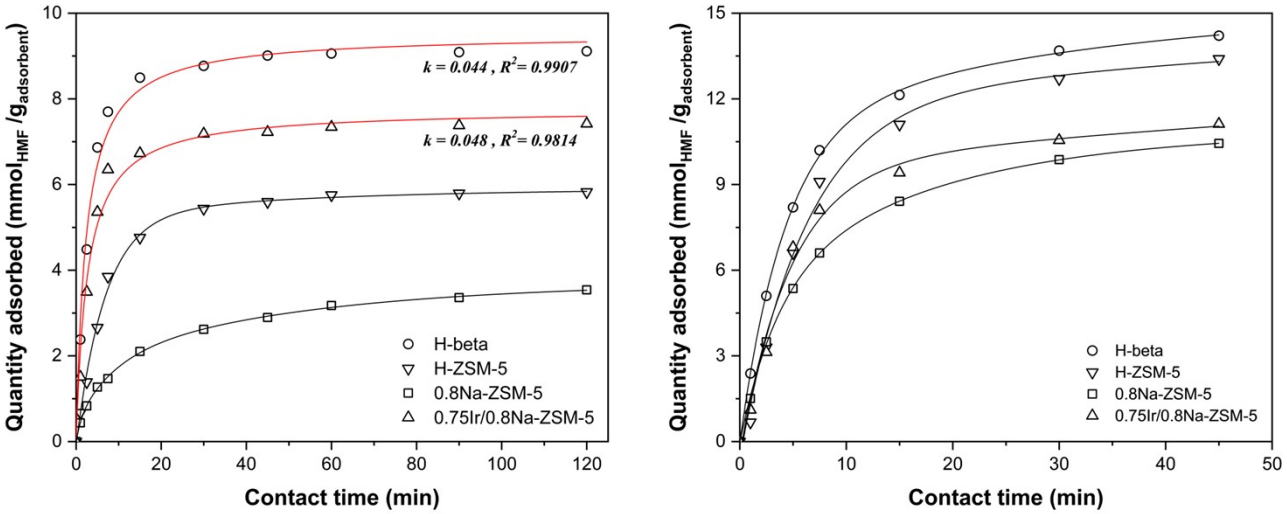


Fig. S5 Adsorption kinetics of HMF and BHMF onto diverse catalysts samples. For the adsorption study of HMF onto diverse catalysts samples, H-beta showed highest adsorption capacity of HMF, confirming its strong affinity towards HMF, which is unfavorable for HMF conversion in a high selectivity manner. The introduction of Ir species significantly increase the adsorption towards HMF. For the adsorption study of BHMF onto diverse catalysts samples, BHMF showed preferential adsorption on all materials, even for Na-modified H-ZSM-5 support, indicating the strong affinity of BHMF to all kinds of acidic materials, which explained the instability of BHMF in acidic environment.

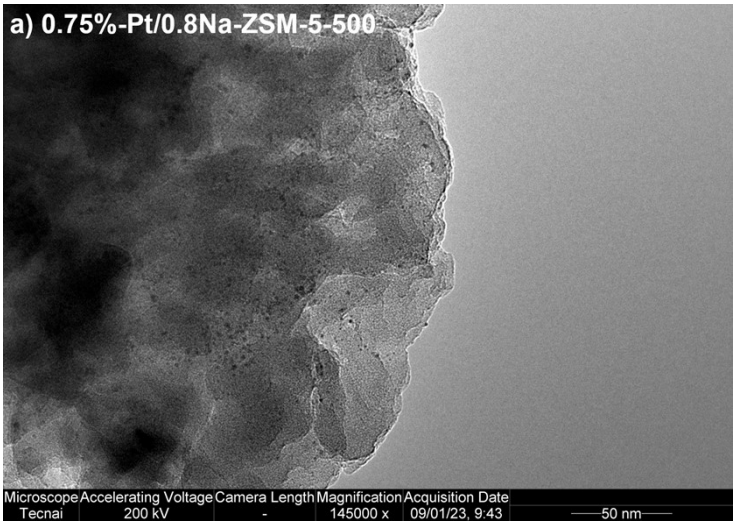


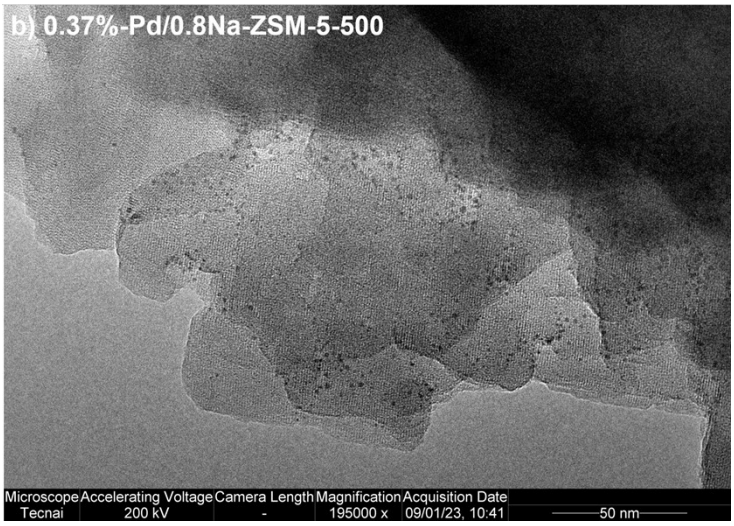


Fig. S6 HR-TEM images of (a) 0.75%-Pt/0.8Na-ZSM-5, (b) 0.37%-Pd/0.8Na-ZSM-5 and (c) 0.37%-Ru/0.8Na-ZSM-5.

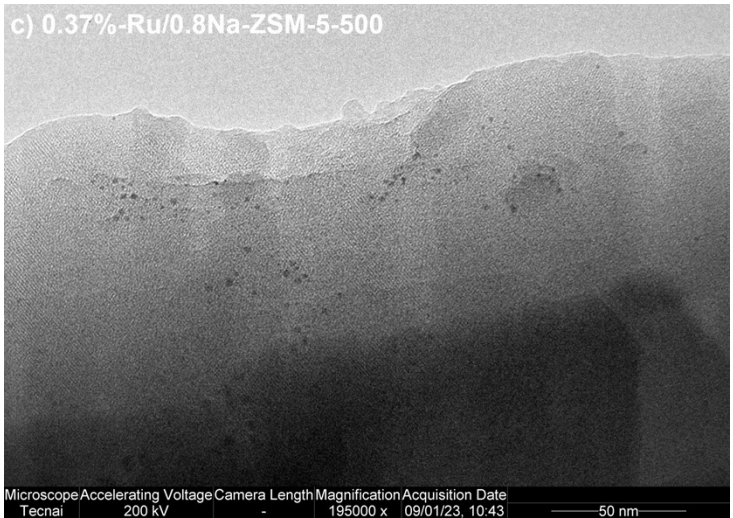

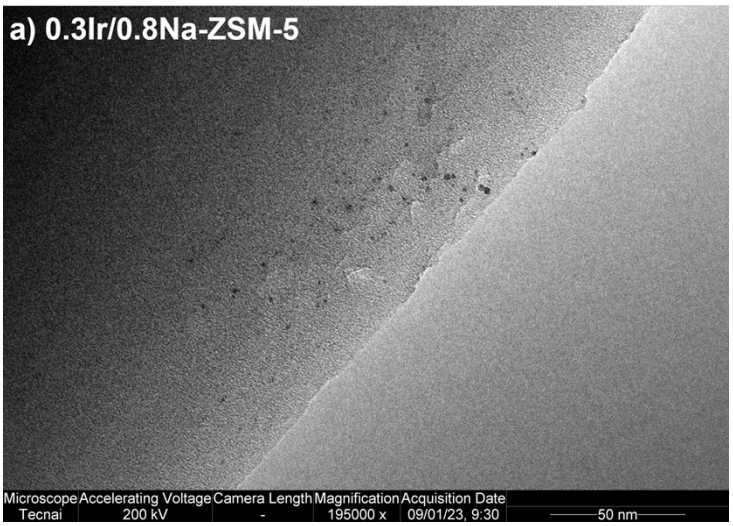
a) 0.3Ir/0.8Na-ZSM-5
Microscope Accelerating Voltage Camera Length Magnification Acquisition Date
Tecnai 200 kV - 195000 x 09/01/23, 9:30
50 nm

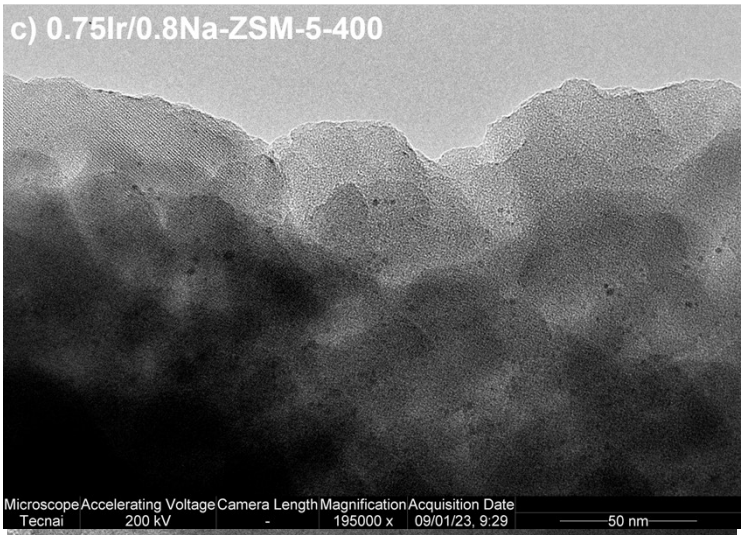
c) 0.75Ir/0.8Na-ZSM-5-400
Microscope Accelerating Voltage Camera Length Magnification Acquisition Date
Tecnai 200 kV - 195000 x 09/01/23, 9:29
50 nm

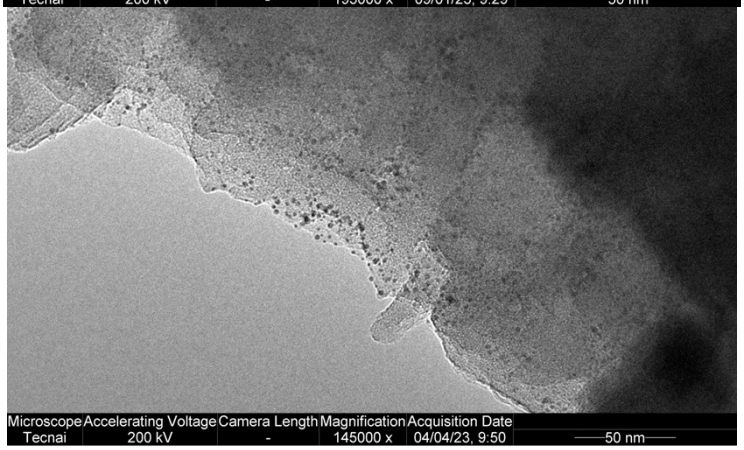
Microscope Accelerating Voltage Camera Length Magnification Acquisition Date
Tecnai 200 kV - 145000 x 04/04/23, 9:50
50 nm

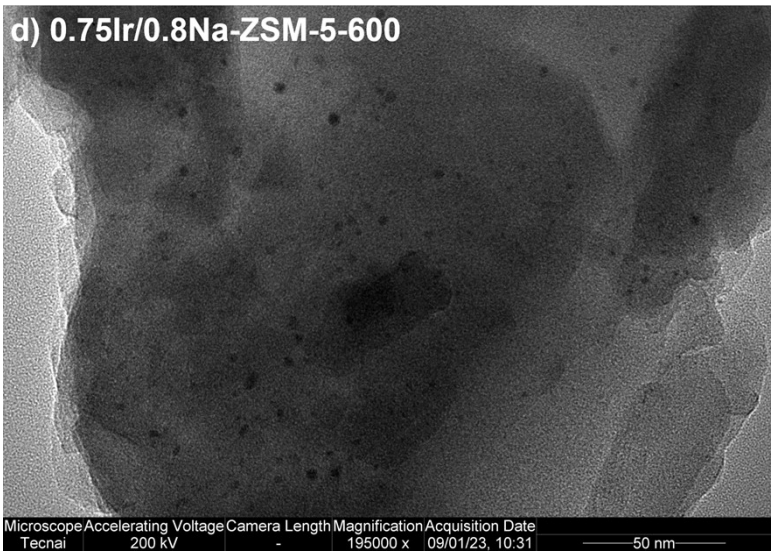


Fig. S7 HR-TEM images of (a) 0.3Ir/0.8Na-ZSM-5-500, (b) 0.75Ir/0.8Na-ZSM-5-300, (c) 0.75Ir/0.8Na-ZSM-5-400 and (d) 0.75 /0.8Na-ZSM-5-600. It is observed that (a) 0.3Ir/0.8Na-ZSM-5-500 exhibited uniformly and highly-dispersed Ir particles of ca. 1.5 nm in particle size. (b) 0.75Ir/0.8Na-ZSM-5-300 and (c) 0.75Ir/0.8Na-ZSM-5-400 represented the similar features of 0.75Ir/0.8Na-ZSM-5-500. Notably, (d) 0.75Ir/0.8Na-ZSM-5-600 showed aggregated Ir particles of ca. 2-3 nm in particle size.

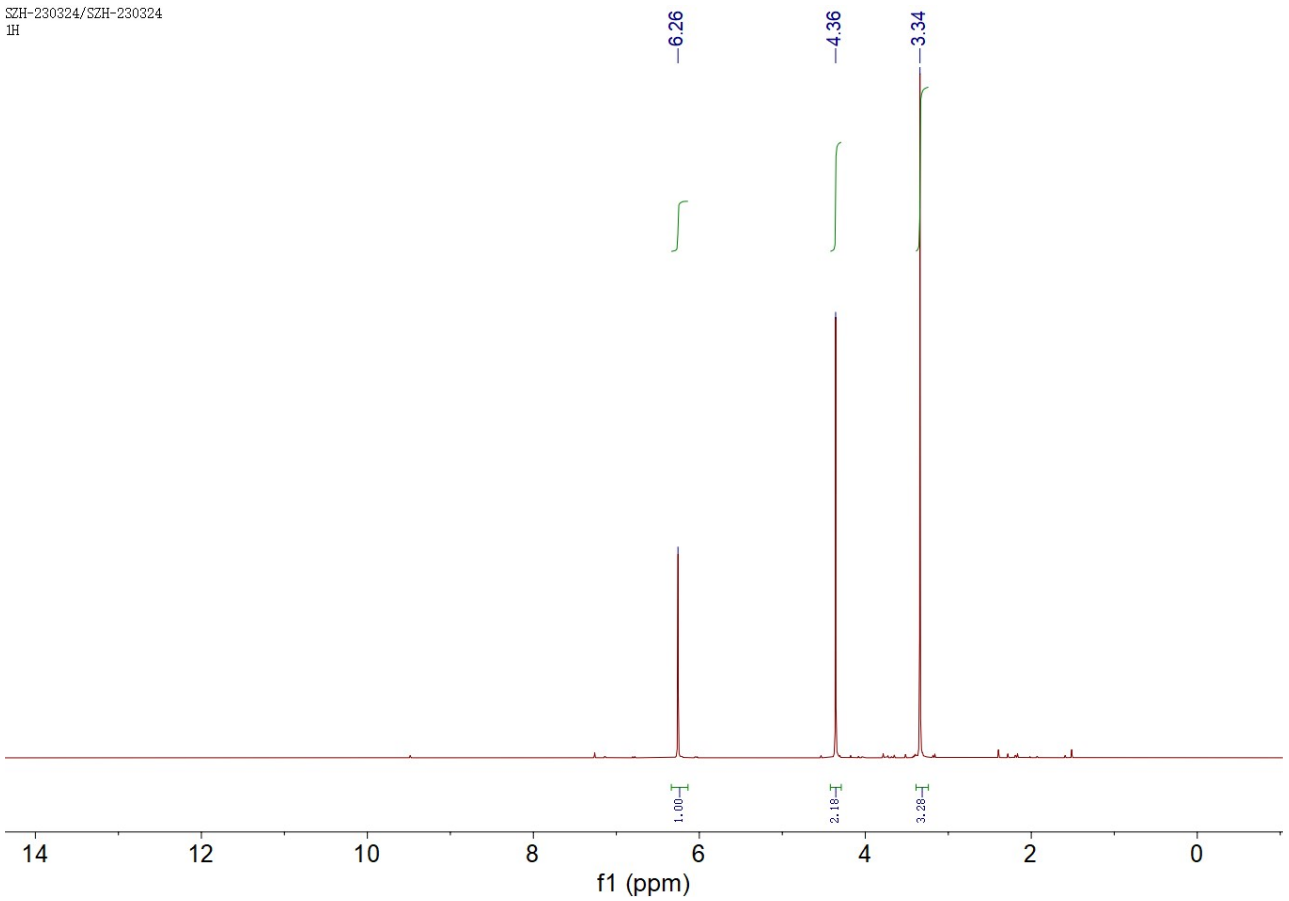


Fig. S8 $^{1}$H-NMR spectra of purified BMMF from reaction mixture and separated BMMF from reaction mixture

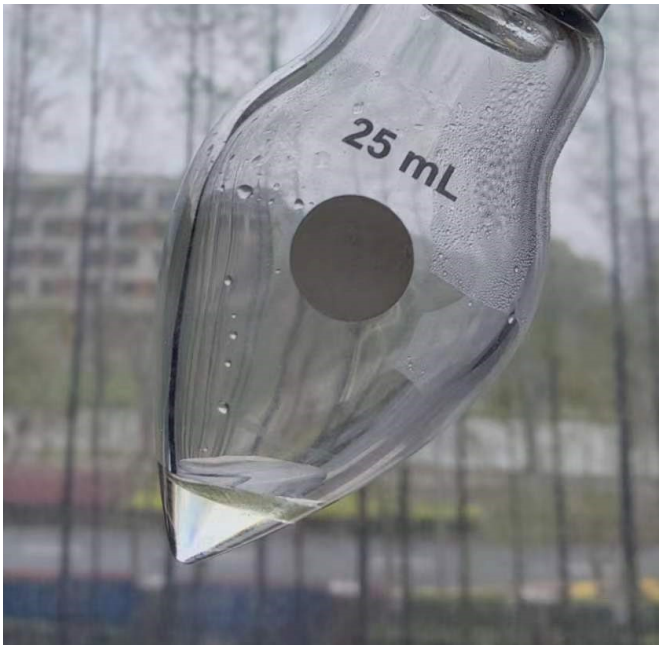

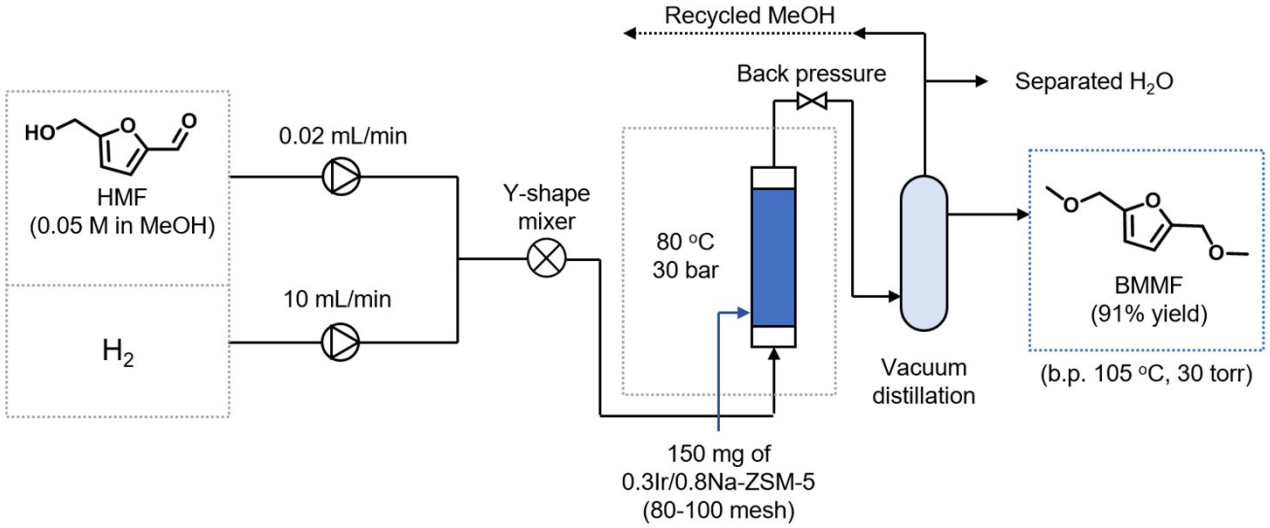


Fig. S9 Diagram for reductive etherification of HMF in flow-reaction mode.

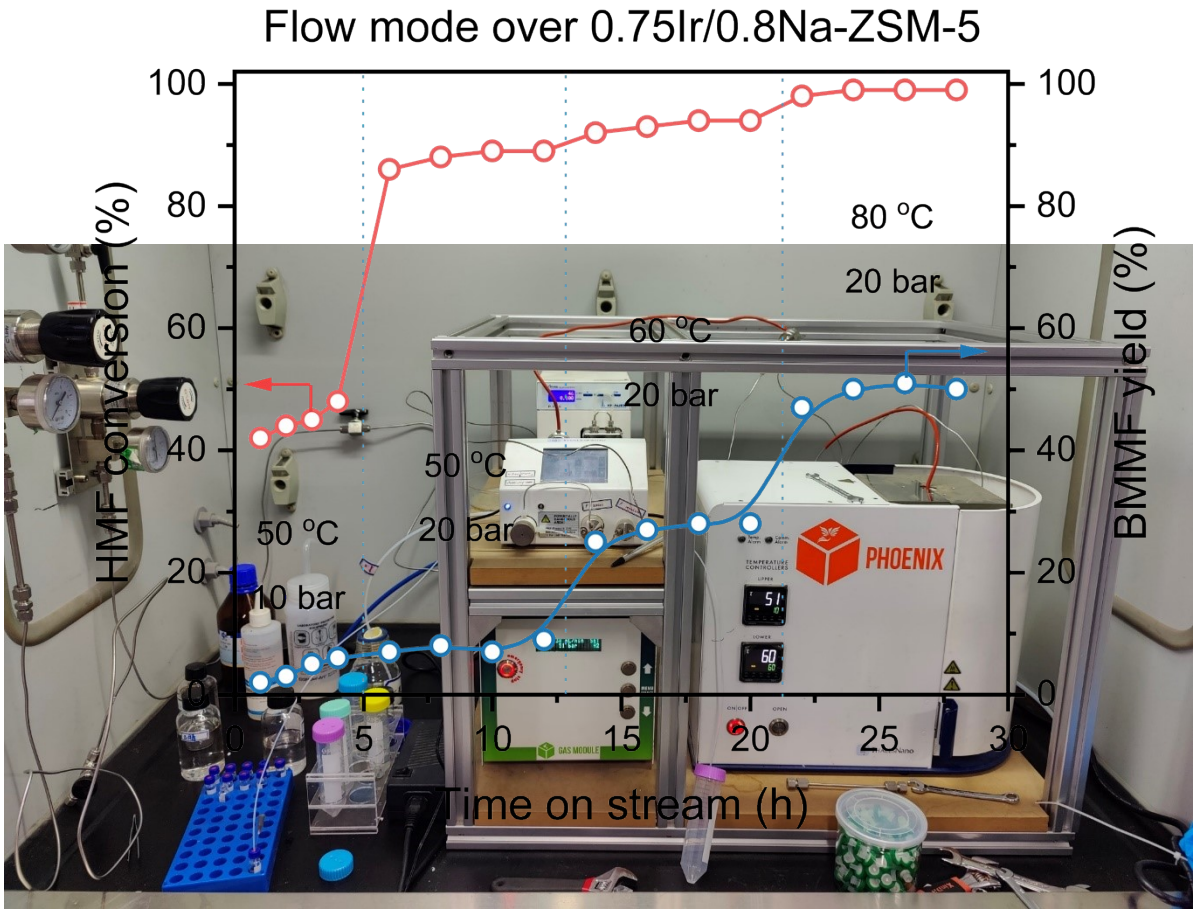

Fig. S10 Reaction conditions optimization for reductive etherification of HMF in flow-reaction mode. Reaction condition: 0.05 M of HMF in MeOH, 150 mg catalyst (0.75Ir/0.8Na-ZSM-5, 80-100 mesh), flow rate of 0.02 mL/min. The reaction condition for reductive etherification of HMF in flow-reaction mode was explored. Slightly increased temperature and $H_2$ pressure was required due to the decrease of exposed sites caused by prilling, emphasizing the importance of abundance of medium-strength - acidity for efficient etherification. As a result, 0.3Ir/0.8Na-ZSM-5 was employed instead of 0.75Ir/0.8Na-ZSM-5.

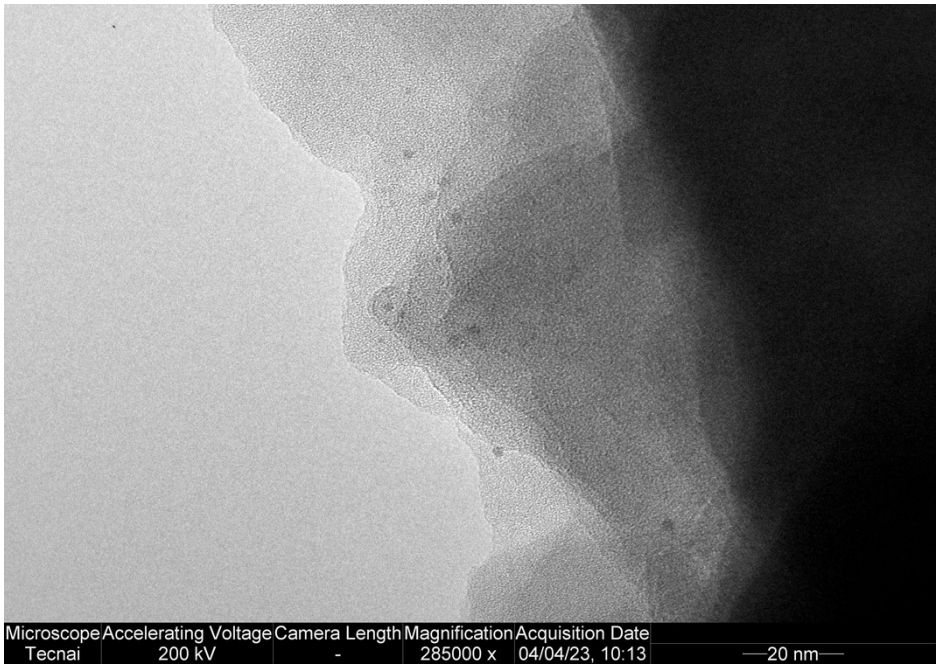


Fig. S11 TEM image of recycled 0.3Ir/0.8Na-ZSM-5 in flow-reaction mode. It is noticed that the basic structure of 0.3Ir/0.8Na-ZSM-5 remain unchanged after 200-h continuous reaction, demonstrating the stability of 0.3Ir/0.8Na-ZSM-5.

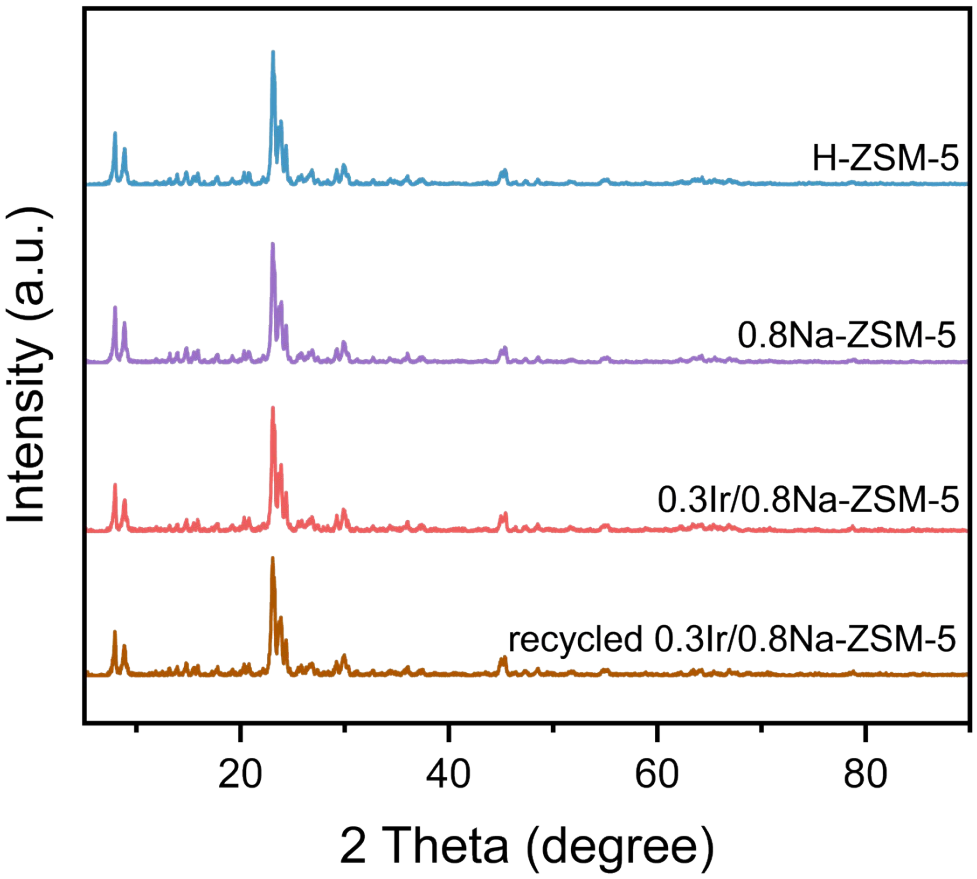
H-ZSM-5
0.8Na-ZSM-5
0.3Ir/0.8Na-ZSM-5
recycled 0.3Ir/0.8Na-ZSM-5
Intensity (a.u.)
20
40
60
80
2 Theta (degree)

Fig. S12 XRD patterns of H-ZSM-5 and recycled 0.3Ir/0.8Na-ZSM-5 in flow-reaction mode. The XRD results proved that the basic structure of ZSM-5 remains unchanged after alkali-modification and reduction. Furthermore, the structure of 0.3Ir/0.8Na-ZSM-5 was preserved after four times of recycle. Notably, no diffraction peak of Ir or $IrO_x$ was observed, indicating the dispersed feature of Ir species.

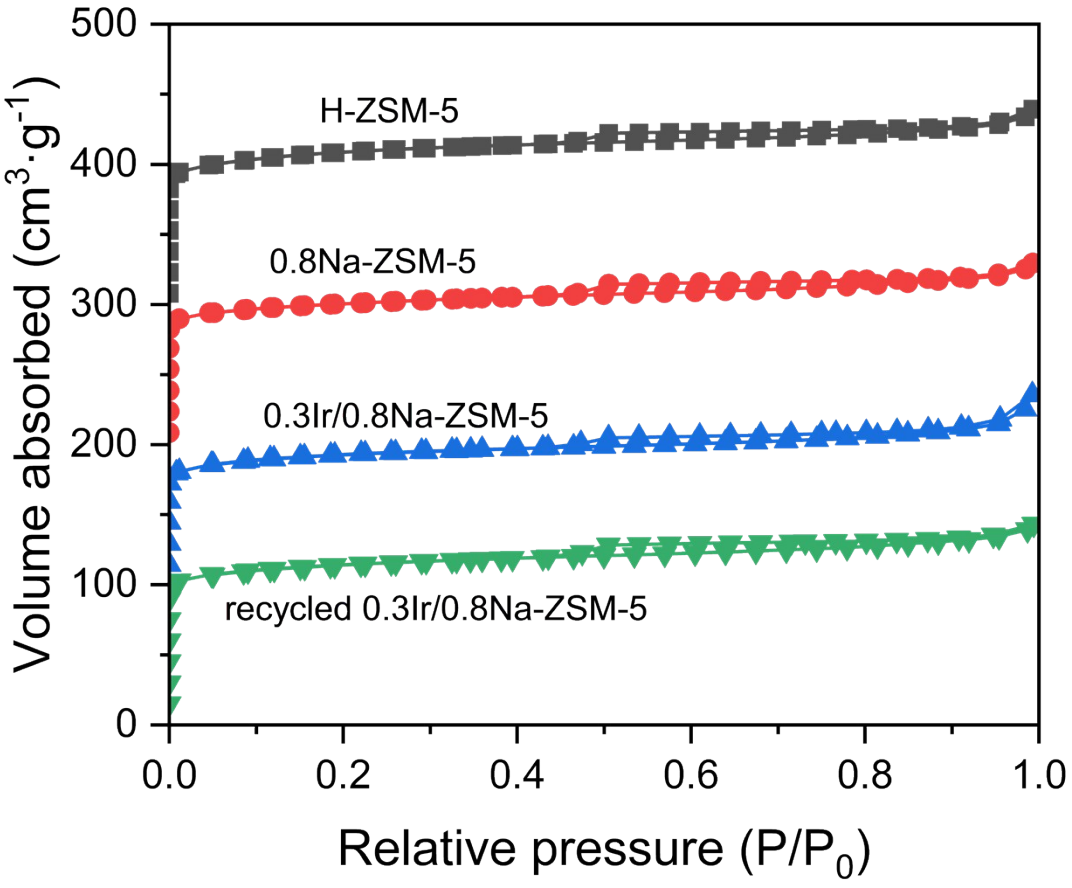

Fig. S13 $N_2$ adsorption and desorption isotherms of reductive etherification of H-ZSM-5, 0.8Na-ZSM-5, 0.75Ir/0.8Na-ZSM-5 and recycled 0.8Na-ZSM-5

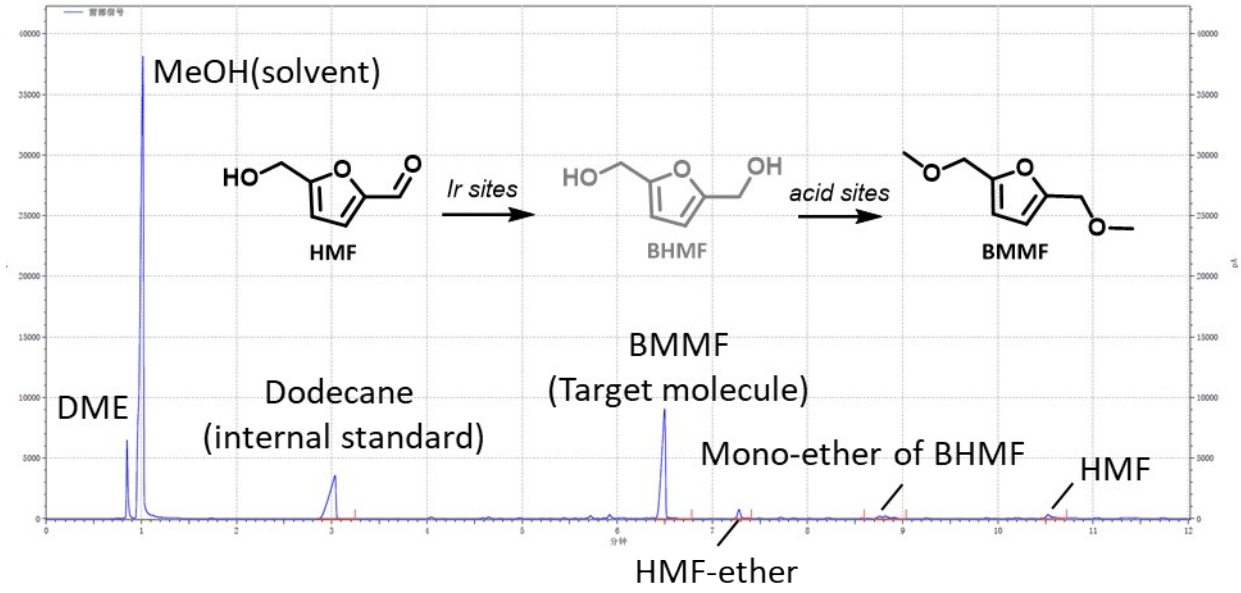


Fig. S14 GC chart of reductive etherification of HMF into BHMF

## 6. References:


1. M.-M. Zhu, X.-L. Du, Y. Zhao, B.-B. Mei, Q. Zhang, F.-F. Sun, Z. Jiang, Y.-M. Liu, H.-Y. He and Y. Cao, *ACS Catalysis*, 2019, **9**, 6212-6222.
2. T. C. Keller, K. Desai, S. Mitchell and J. Pérez-Ramírez, *ACS Catalysis*, 2015, **5**, 5388-5396.
3. C. Hammond, S. Conrad and I. Hermans, *Angewandte Chemie International Edition*, 2012, **51**, 11736-11739.
4. M. Musolino, M. J. Ginés-Molina, R. Moreno-Tost and F. Aricò, *ACS Sustain. Chem. Eng.*, 2019, **7**, 10221-10226.
5. D. Gupta and B. Saha, *Catal. Commun.*, 2018, **110**, 46-50.
6. Y.-S. Lee, J. Kim, J. Han, Y.-H. Kim, B. Jung, S. Hwang and J. Jegal, *Synlett*, 2017, **28**, 2299-2302.
7. Q. Cao, W. Liang, J. Guan, L. Wang, Q. Qu, X. Zhang, X. Wang and X. Mu, *Appl. Catal. A Gen.*, 2014, **481**, 49-53.
8. W. Fang, H. Hu, P. Dong, Z. Ma, Y. He, L. Wang and Y. Zhang, *Applied Catalysis A: General*, 2018, **565**, 146-151.
9. M. Balakrishnan, E. R. Sacia and A. T. Bell, *Green Chem.*, 2012, **14**, 1626–1634.
10. J. Wei, T. Wang, X. Cao, H. Liu, X. Tang, Y. Sun, X. Zeng, T. Lei, S. Liu and L. Lin, *Appl. Catal. B Environ.*, 2019, **258**, 117793.
11. X.-L. Li, K. Zhang, S.-Y. Chen, C. Li, F. Li, H.-J. Xu and Y. Fu, *Green Chem.*, 2018, **20**, 1095-1105.
12. Y. Yang, H. Hu, Q. Fang, G. Lu, H. He, H. Chen, C. Chen and J. Zhang, *Catalysis Today*, 2023, **423**, 114290.
13. B. Liu, Y. Nakagawa, C. Li, M. Yabushita and K. Tomishige, *ACS Catal.*, 2022, **12**, 15431-15450.